Supporting Information for:

Hydrogen Generation Catalyzed by Fluorinated Diglyoxime-Iron Complexes at Low Overpotentials

Michael J. Rose, Harry B. Gray and Jay R. Winkler*

Beckman Institute, California Institute of Technology; Pasadena, CA 91125

Supporting Information Contents **Page**

Materials and Methods

Reagents and Procedures. Hydroxylamine hydrochloride, glyoxal (as 40% wt aqueous solution), Cl_2 gas and bromopentafluorobenzene were obtained from Sigma-Aldrich chemical company. Diglyoxime (dH_2gH_2) and dichloroglyoxime (dCl_2gH_2)[1] were synthesized according to published procedures. Batches of pentafluoromagnsium bromide Grignard reagent were either purchased from Novel Chemical Solutions, or generated by the published method of Zhen and co-workers.[2,3] Iron(II) acetate was procured from Sigma-Aldrich and stored under N_2 atmosphere until use. Trifluoroacetic acid, pentane, $CHCl_3$ and MeOH were purchased from J.T. Baker and used without further purification, while all other solvents (MeCN, THF, Et_2O and toluene) were obtained from a solvent purification system according to the method of Grubbs.[4] Deuterated solvents were purchased from Cambridge Isotopes and used as received.

Di(pentafluorophenyl)glyoxime (dAr^FgH_2). Under N_2 atmosphere, 16.0 g (64.8 mmol) of bromopentafluorobenzene was diluted in 60 mL of dry THF and cooled to 0° C. Next, 21.6 mL of a 1 M solution of isopropylmagnesium bromide was diluted in 20 mL of THF. The ^{i}PrMgBr solution was added dropwise to the Ar^FBr at 0° C over the course of 30 min, and allowed to warm to room temperature over 30 min. The mixture was again cooled to 0° C, and a batch of dichloroglyoxime dihydrochloride (3.73 g, 16.2 mmol) dissolved in 30 mL of THF was added via cannula over 1 hr to generate a light orange solution. The solution was allowed to stir for an additional 1 h at 0° C, then allowed to warm to room temperature over 12 h. The resulting dark red solution was then concentrated to ~20 mL and poured into a stirred solution of NH_4Cl (5 g) in 60 mL of water. The THF was evaporated to afford a beige solid that was collected by filtration, and the product recrystallized from MeOH/H_2O to afford a white to beige solid. Yield: 4.41 g (54%). ^{1}H NMR (d^8-THF), δ from TMS: 11.86 s (2H N-OH). ^{19}F NMR (d^8-THF), δ from $CFCl_3$: −137.4 d (2 F), −153.8 t (1 F), −163.5 m (2 F). ^{13}C NMR (d^8-THF), δ from TMS: 146.9 (4 C), 143.4 (4 C), 141.2 (2 C), 137.7 (2 C), 109.8 (2 C). Selected IR bands in cm^{-1} (KBr disc): 3281 w (O-H), 1658 m (C=N), 1527 m, 1508 s, 1445 m, 1158 m, 1148 w, 1034 m, 989 s, 952 s, 833 s.

[$(dAr^FgH)_2Fe(py)_2$] (1). The ligand dAr^FgH_2 (2.0 g, 4.0 mmol) was dissolved in 40 mL of MeCN containing 322 mg (4.0 mmol) of pyridine. Fe^{II}(acetate) (952 mg, 0.20 mmol) was added to the stirred solution of ligand. Over the course of 10 min, a violet color developed and was allowed to stir for an additional 2 hours. A violet microcrystalline solid was collected by filtration and washed thoroughly with Et_2O. Yield: 1.77 g (73%). X-ray quality crystals of **1** were grown via vapor diffusion of pentane into a concentrated solution of **1** in $CHCl_3$ at room temperature. ^{1}H NMR (CD_2Cl_2), δ from TMS: 8.40 d (4 H), 7.69 t (2 H), 7.19 t (4 H); ^{19}F NMR (CD_2Cl_2), δ from $CFCl_3$: −138.5 d (8 F), −151.5 t (4 F), −161.5 m (8 F). Anal. calcd. for $C_{38}H_{12}N_6O_4F_{20}Fe$: C 43.37, H 1.15, 7.99; found: C 44.11, H 1.03, N 8.16. Selected IR bands in cm^{-1} (KBr disc): 1524 s, 1497 s, 1452 w, 1406 m, 1101 m, 993 m, 840 w, 766, 725 w, 695 w. UV/vis in $CHCl_3$, λ in nm (ε in M^{-1} cm^{-1}): 560 (11 200), 350 (10 200), 315 (10 300).

[$(dAr^Fg_2BF_2)_2Fe(py)_2$] (2). This macrocyclic complex was synthesized by a procedure analogous to that listed for complex **3** below, except that 6 equiv of BF_3•Et_2O (200 μL, 2.90 mmol) were used and the reaction was allowed to stir for 4 h at room temperature. After the extraction, vapor diffusion of pentane into a violet solution of **3** in $CHCl_3$ afforded violet needles suitable for X-ray diffraction. Yield: 52 mg (24%). ^{1}H NMR ($CDCl_3$), δ from TMS: 7.98 d (4 H), 7.73 t (2 H), 7.23 t (4 H); ^{19}F NMR ($CDCl_3$), δ from $CFCl_3$: −137.2 d (8 F), −146.0 t (4 F), −146.6 (4 F), −158.3 m (8 F). Anal. calcd. for $C_{38}H_{10}N_6O_4F_{24}FeB_2$: C 39.76, H 0.88, 7.32; found: C 39.55, H 0.94, N 7.34. Selected IR bands in cm^{-1} (KBr disc): 1558 w, 1530 m, 1508 m, 1503 s, 1421 w, 1201 w, 1110 s, 1017 s, 895 w, 838 m, 720 w. UV/vis in $CHCl_3$, λ in nm (ε in M^{-1} cm^{-1}): 570 (14 700), 340 sh (7 770).

[(dAr^{F}g$_2$-H-BF$_2$)Fe(py)$_2$] (3). A batch of violet **1** (0.220 g, 0.181 mmol) was slurried in an Et_2O/MeCN mixture (3:1) at room temperature. Next, 4 equiv of BF_3•Et_2O (200 μL, 1.45 mmol) were added dropwise to the solution over 10 min, generating a maroon slurry that was stirred for 1 h at RT. Filtration of the reaction mixture afforded ~150 mg of unreacted violet starting material. The red filtrate was placed at −20 ℃ to precipitate a colorless py•HF byproduct, which was removed via filtration. The clear red filtrate was then evaporated, and 10 mL of Et_2O added to collect a dark orange solid (115 mg). The solid was dissolved in a solution of 3 mL of $CHCl_3$ containing 2.2 equiv of pyridine (15 mg) to generate a violet solution over 6 h, wherein more colorless crystals of py•HF formed and were filtered. Yield: 43 mg (16%). Vapor diffusion of pentane into the violet $CHCl_3$ solution of **3** afforded violet needles suitable for X-ray diffraction. ^{1}H NMR ($CDCl_3$), δ from TMS: 8.01 d (4 H), 7.63 t (2 H), 7.14 t (4 H); ^{19}F NMR ($CDCl_3$), δ from $CFCl_3$: −137.5 d (4 F), −137.8 d (4 F), −147.7 t (2 F), −147.6 s (2 F), −148.1 t (2 F), −159.3 m (8 F). Anal. calcd. for $C_{38}H_{11}N_6O_4F_{22}FeB$: C 41.49, H 1.01, 7.64; found: C 42.17, H 1.14, N 7.83. Selected IR bands in cm^{-1} (KBr disc): 3428 br (N-OH), 2937 w, 1611 m, 1529 m, 1505 s, 1446 w, 1149 w, 1084 m, 989 s, 953 s, 822 s, 580 w. UV/vis in $CHCl_3$, λ in nm (ε in M^{-1} cm^{-1}): 565 (9 780), 350 sh (5 300), 315 sh (6 730).

Physical Measurements. ^{1}H and ^{19}F NMR spectra were collected on a Varian Mercury 300 MHz spectrometer and chemical shifts referenced to TMS (^{1}H, ^{13}C) or $CFCl_3$ (^{19}F). UV/vis absorption spectra were obtained using a Cary 50 spectrophotometer using 0.1 mM solutions in 1 cm quartz cuvettes, and infrared spectra were recorded in KBr disks with a Thermo-Scientific Nicolet 6700 FT-IR spectrometer.

Electrochemistry. Cyclic voltammograms were collecting using a CH Instruments 660 potentiostat using a polished glassy carbon working electrode, platinum counter-electrode, and Ag/AgCl reference electrode in CH_2Cl_2; potentials were referenced versus ferrocene as internal standard, and are plotted versus SCE using the known potential of Fc/Fc^+ vs SCE (+380 mV). Bulk electrolyses (Schlumberger SI 1286 potentiostat) were performed at a fixed potential (−0.95 V vs SCE, referenced internally vs Fc) in 30 mL of MeCN containing 1.3 mM of catalyst and 30 mM TFA in a fritted H-cell using a bundled array of twenty 0.9 mm diameter graphite rods as working electrode; 2 × 8 × 0.5 cm graphite rod as counter-electrode; Ag wire in a fritted glass tube as reference electrode. Faradaic yields were determined by mannometry using a mercury capillary apparatus; the presence of headspace H_2 was confirmed by gas chromatography using an Agilent Technologies 7890A GC System equipped with a TCD.

X-ray Diffraction Data Collection and Crystal Structure Refinement. Crystals were mounted on a glass fiber using Paratone oil then placed on the diffractometer under a stream of N_2 at 100 K. Refinement of F^2 against all reflections: the weighted R-factor (*w*R) and goodness of fit (S) were based on F^2, conventional R-factors (R) were based on F, with F set to zero for negative F^2. The threshold expression F2 > 2σ (F^2) was used only for calculating R-factors(gt) and was not relevant to the choice of reflections for refinement. Diffraction intensity data were collected on a Bruker Kappa APEX II diffractometer equipped with a MoKα X-ray source and data were collected using APEX2 v2009.7-0; the data reduction program SAINT-plus v7.66A was used. In the case of complexes **1** and **2**, the H-bonded NO-H-ON hydrogens were located in the difference map and refined isotropically, while all other hydrogens were fixed according to standard parameters in SHELXL.

References

(1) Lance, K. A., Goldsby, K. A., Busch, D. H. *Inorg. Chem.* **1990**, *29*, 4537-4544.
(2) Song, L., Hu, J., Wang, J., Liu, X., Zhen, Z. *Photochem. Photbiol. Sci.* **2008**, *7*, 689-693.
(3) Wall, L. A., Donadio, R. E., Pummer, W. J. *J. Am. Chem. Soc.* **1960**, *82*, 4846.
(4) Pangborn, A. B., Giardello, M. A., Grubbs, R. H., Rosen, R. K., Timmers, F. J. *Organometallics* **1996**, *15*, 1518.

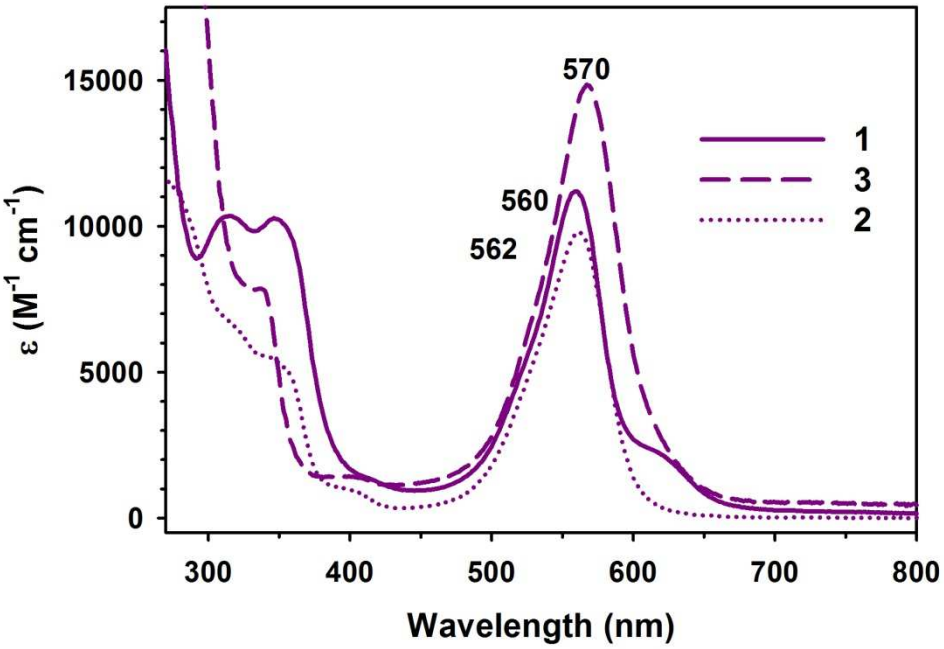

Figure S1. UV/vis absorption spectra of **1**-**3** in $CHCl_3$ at 298 K.

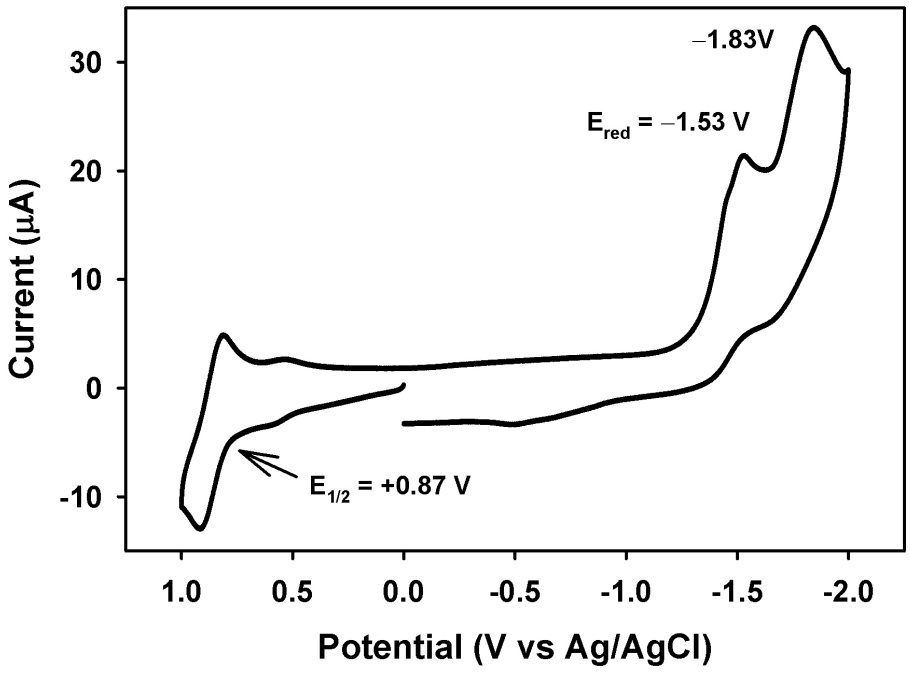

Figure S2. Cyclic voltammogram of **1** recorded in MeCN. Experiment parameters: 0.1 M NBu_4ClO_4, glassy carbon WE, Pt CE, Ag/AgCl RE, recorded under Ar atmosphere at 298 K.

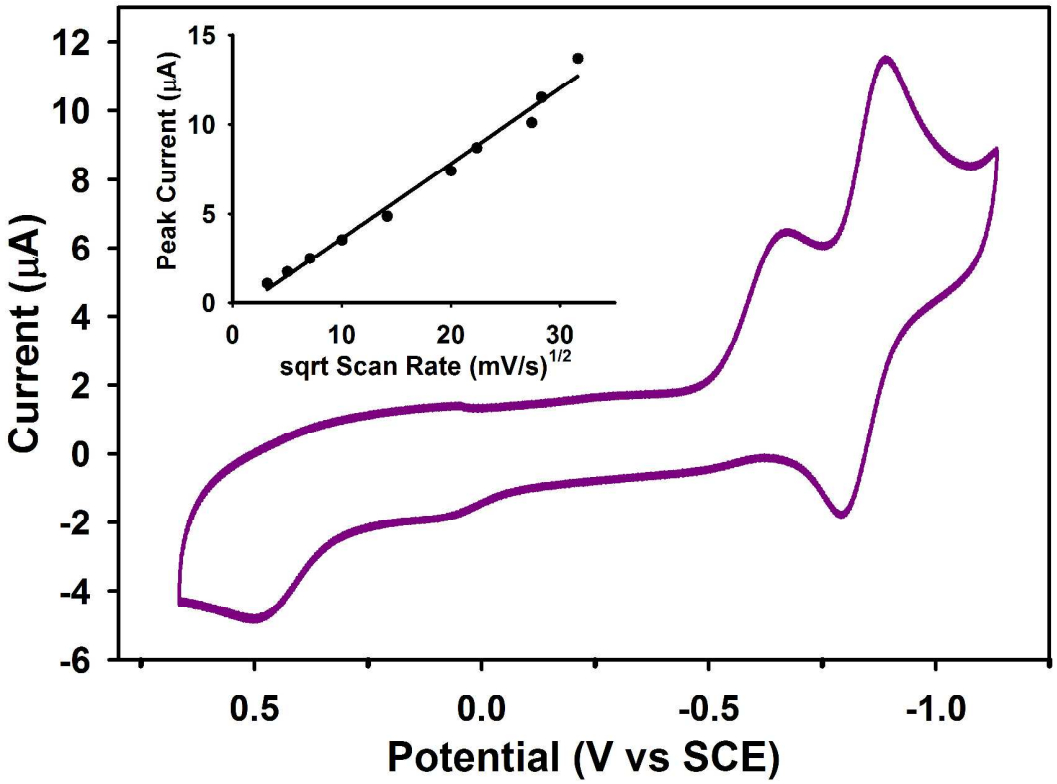

Figure S3. CV of **2** in CH_2Cl_2 solution under an Ar atmosphere. Experimental parameters: 100 mV/s; [**2**] = 0.5 mM; 0.1 M NBu_4ClO_4, GC WE, Pt CE, Ag/AgCl RE (internally referenced versus ferrocene).

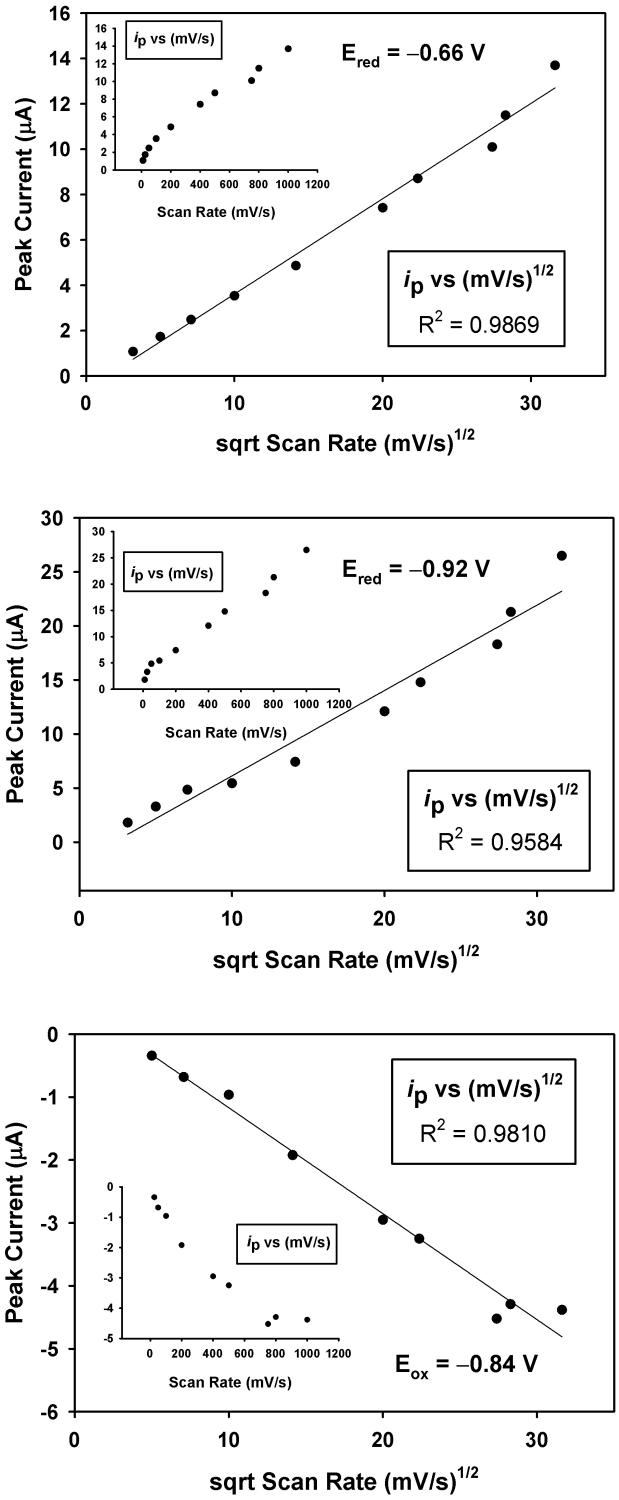

Figure S4. Scan rate dependence of the reduction (top two panels) and oxidation (bottom panel) features in cyclic voltamograms of **2** in CH_2Cl_2. Experiment parameters: 0.1 M NBu_4ClO_4, glassy carbon WE, Pt CE, Ag/AgCl RE, recorded under Ar atmosphere at 298 K.

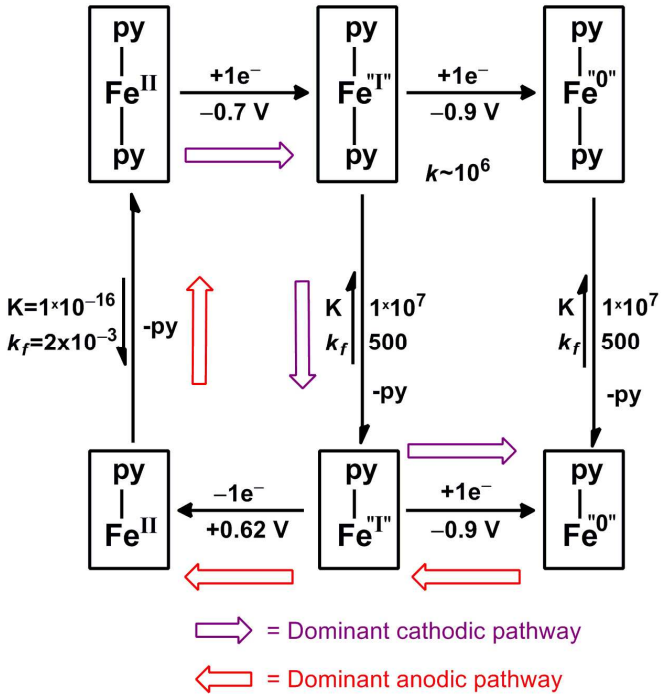

Scheme S1A. Electrochemical/chemical model for **2** including kinetic and thermodynamic parameters resulting from CV simulations.

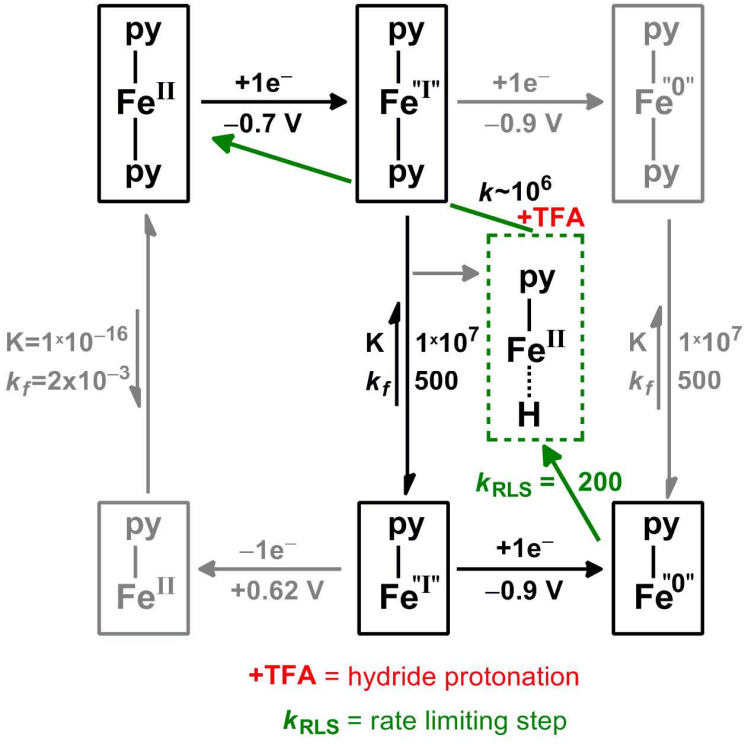

Scheme S1B. Catalytic model for **2** including kinetic and thermodynamic parameters resulting from CV simulations. Intermediates and values shown in gray were simulated, but found not to contribute significantly to catalysis: k_{RLS} (M^{-1} s^{-1}).

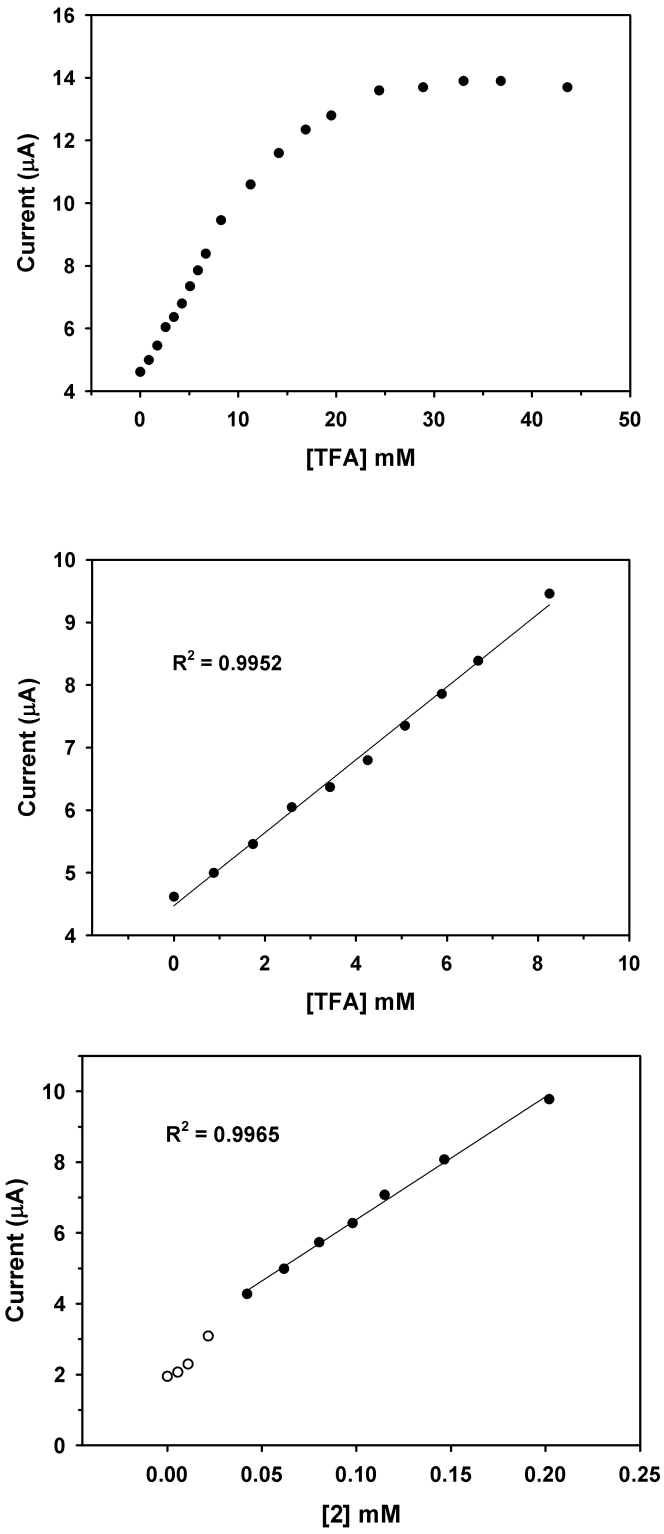

Figure S5. Electrocatalytic current dependence on the entire range of [TFA] (top), on the linear range of [TFA] (middle), and on catalyst concentration [**2**] (bottom) in cyclic voltammetry experiments with **2** in CH_2Cl_2. Experiment parameters: 0.1 M NBu_4ClO_4, glassy carbon WE, Pt CE, Ag/AgCl RE, recorded under Ar atmosphere at 298 K.

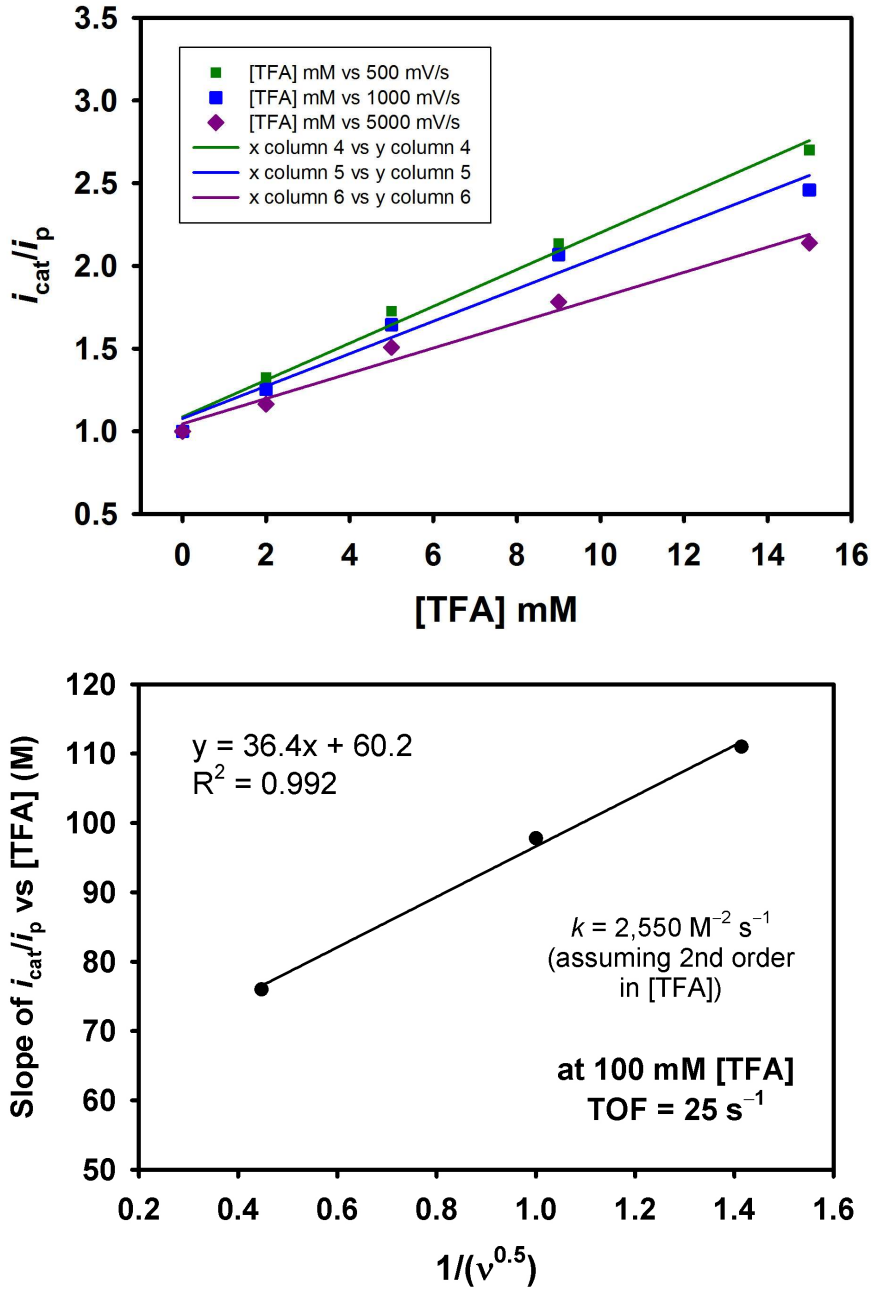

Figure S6. (Top) Dependence of i_{cat}/i_p on [TFA] in the linear region at high scan rates for **2**. (Bottom) Analysis of the resulting slopes (i_{cat}/i_p vs [TFA] in the linear region) assuming a second-order dependence on [TFA] affords rate constant as indicated. The resulting turnover frequency (TOF) calculated at 100 mM [TFA] is nearly identical to that provided by analysis of simulated CVs (see text, and below). Experiment parameters: 0.1 M NBu_4ClO_4, glassy carbon WE, Pt CE, Ag/AgCl RE, recorded under Ar atmosphere at 298 K.

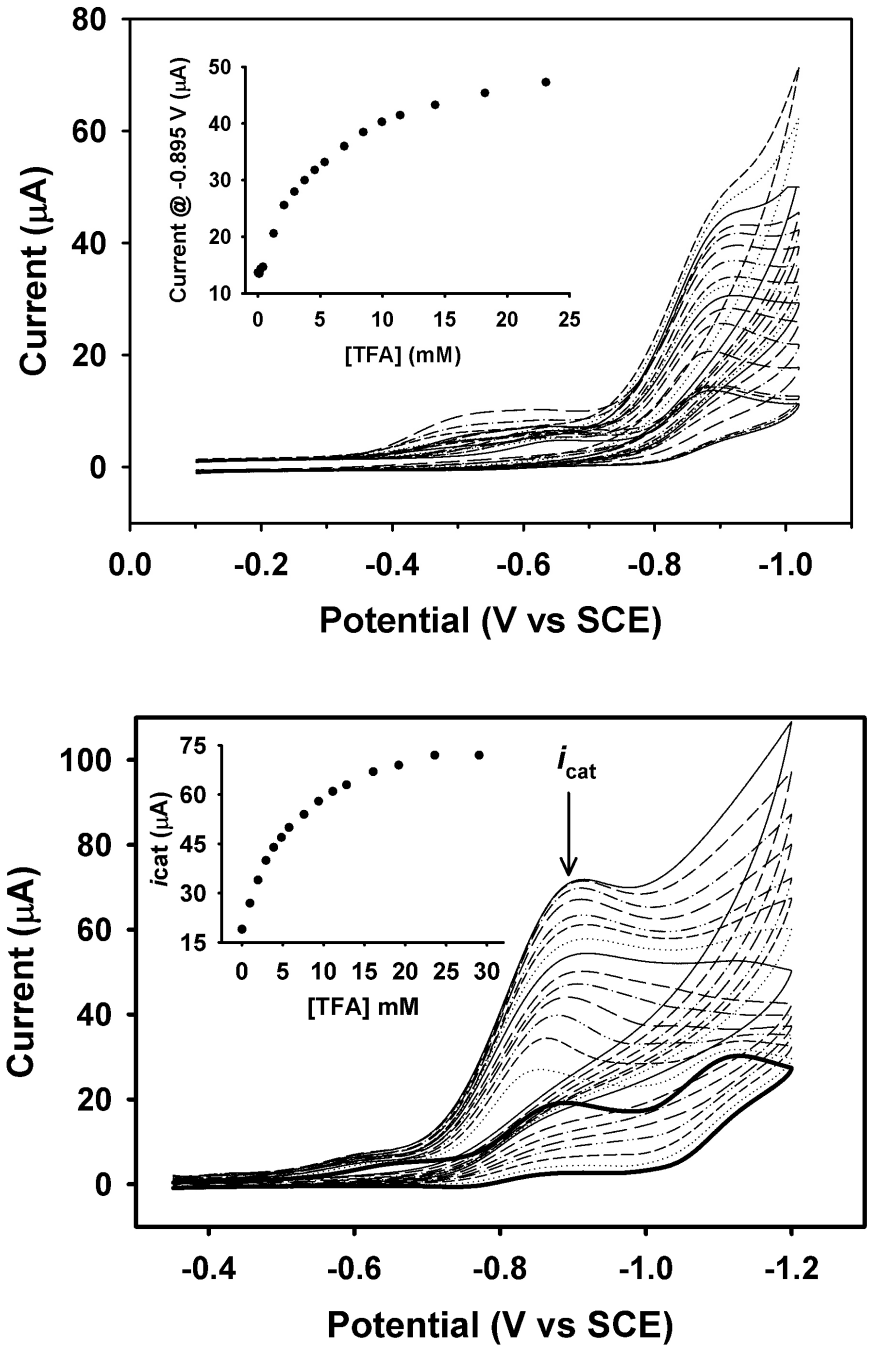

Figure S7. Cyclic voltammograms of **2** (top) and **3** (bottom) in MeCN in the presence of increasing concentrations of TFA. Inset: Peak catalytic currents plotted versus [TFA]. Experiment conditions: 0.1 M NBu_4ClO_4; scan rate: 100 mV/s; WE: glassy carbon; CE: platinum wire; RE: 0.01 M $Ag/AgNO_3$ in MeCN. Potentials were referenced vs ferrocene as the internal standard and are plotted vs SCE.

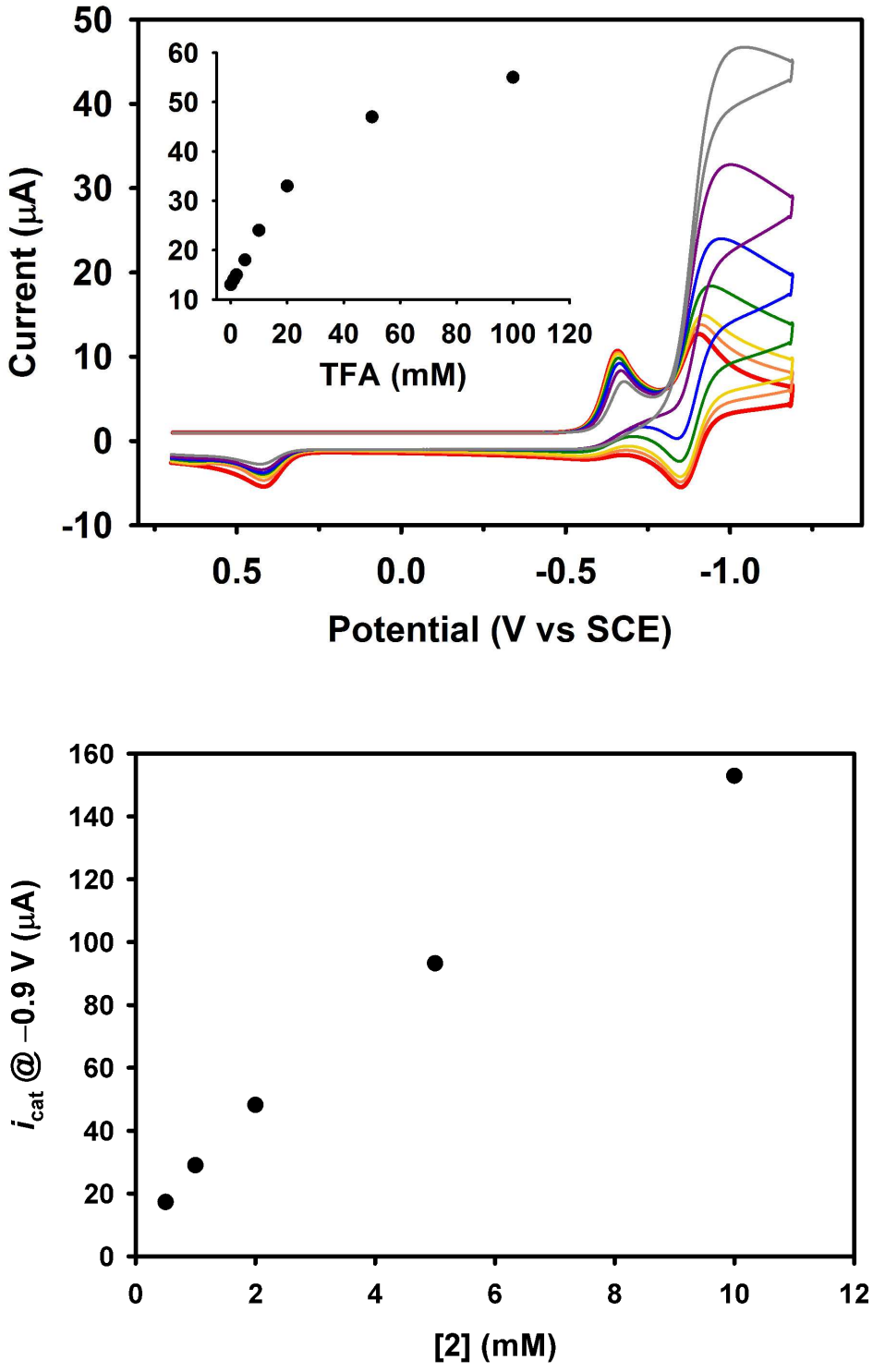

Figure S8. *Top:* Simulated CVs of **2** in the presence of increasing [TFA]. Bottom: Simulated linear dependence of i_{cat} on [**2**]. Simulation parameters: [**2**] = 1 mM, [TFA] = 0-50 mM; scan rate = 100 mV/s; capacitance = 1×10^{-5} F. Kinetic and thermodynamic parameters listed in Scheme S1.

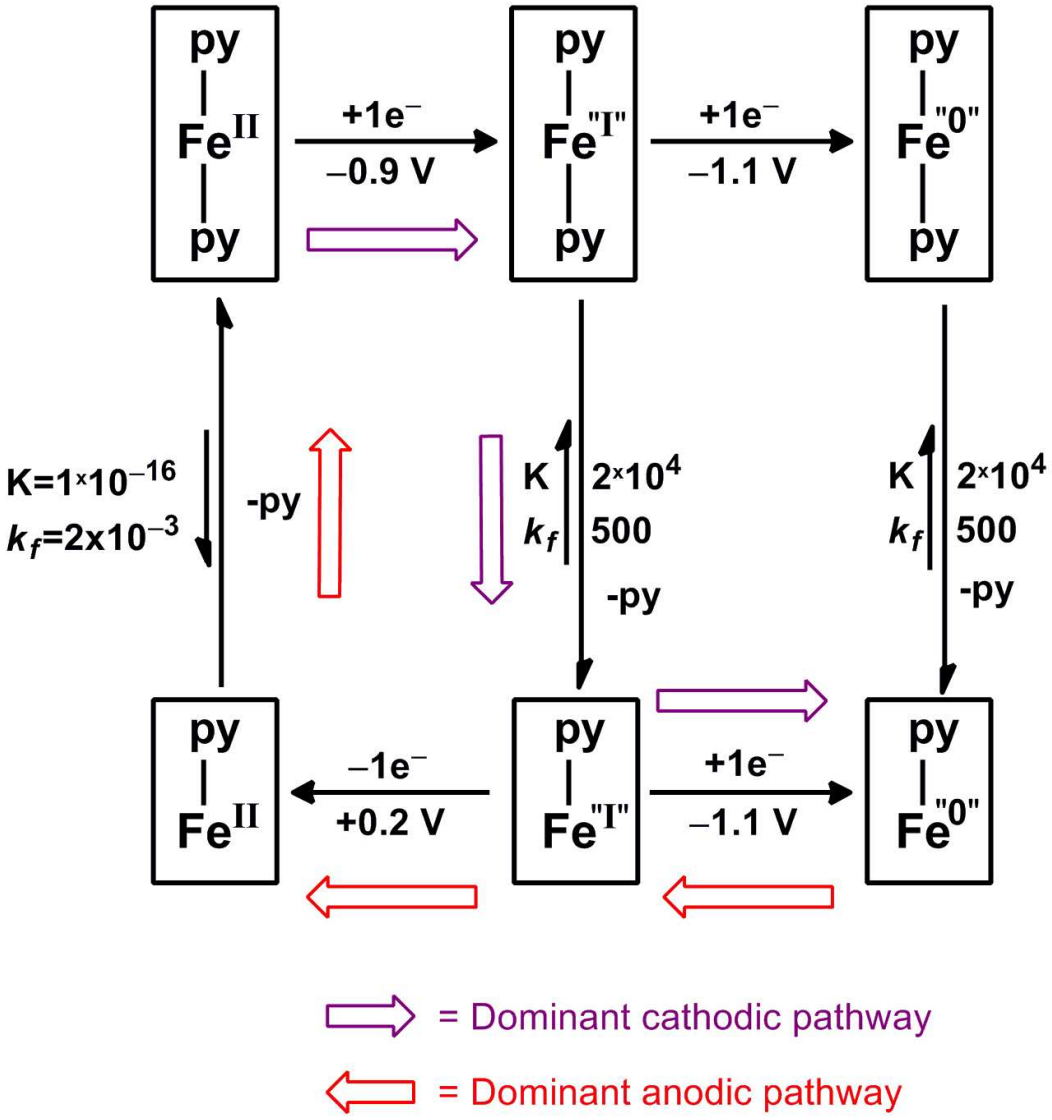

Scheme S2A. Electrochemical/chemical model for CVs of **3** (no acid) including kinetic and thermodynamic parameters resulting from CV simulations.

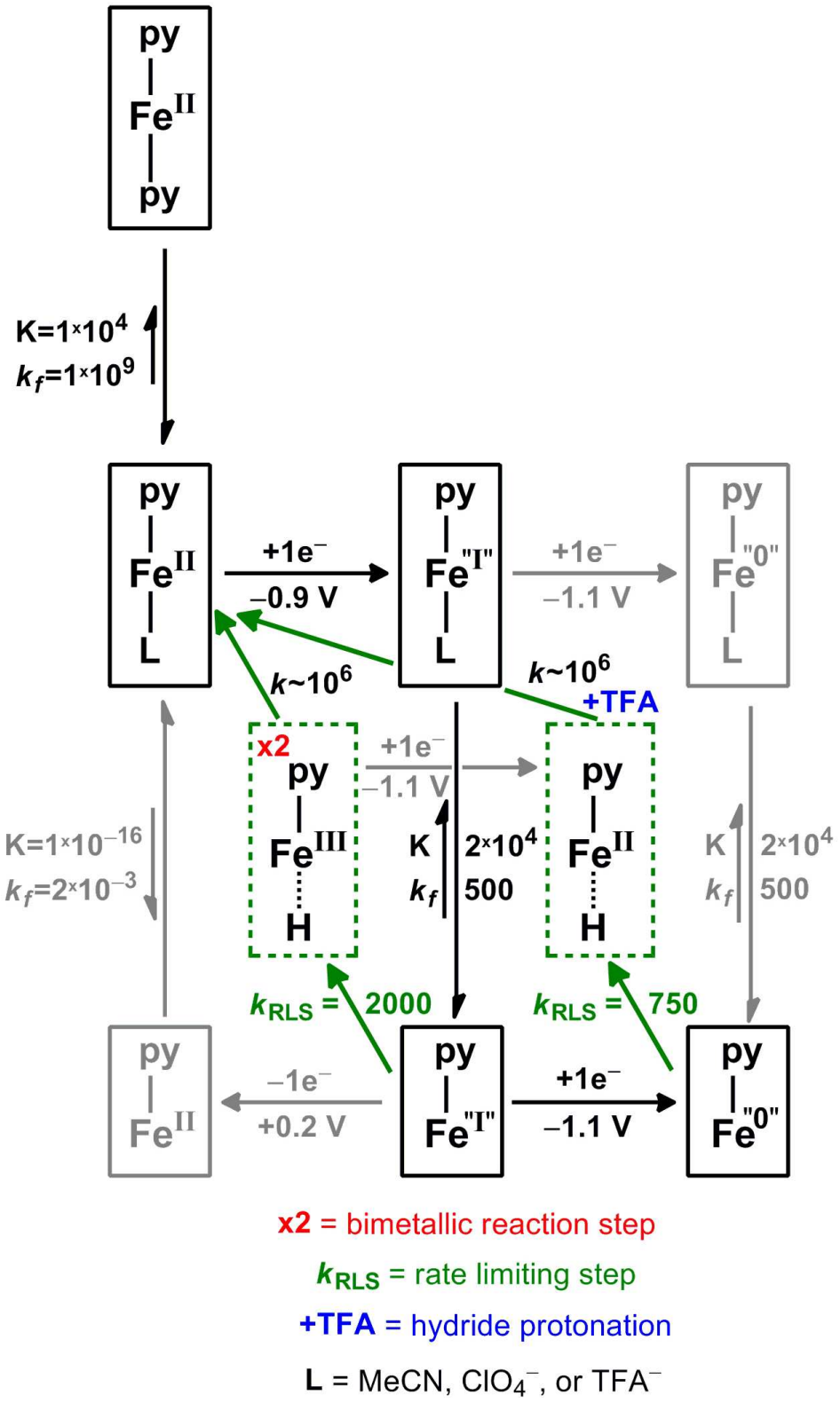

Scheme S2B. Catalytic model for **3** including kinetic and thermodynamic parameters resulting from CV simulations. Intermediates and values shown in gray were simulated, but found not to contribute significantly to catalysis: k_{RLS} (M^{-1} s^{-1}).

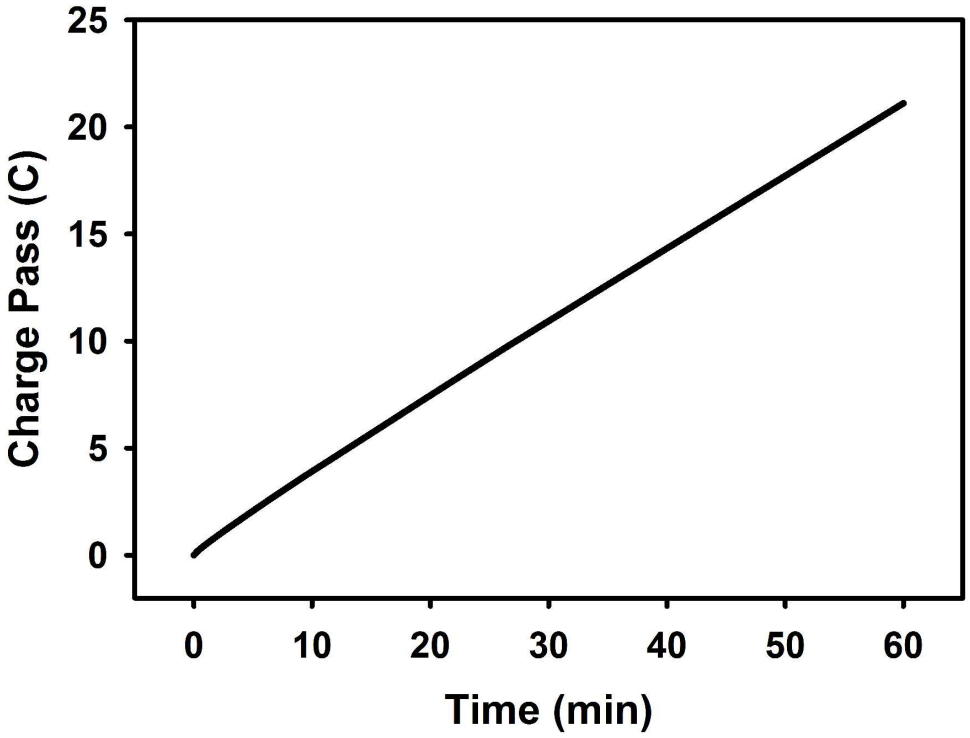

Figure S9. Bulk electrolysis for H_2 generation using [(dArFg$_2$-H-BF$_2$)Fe(py)$_2$] (**3**) in MeCN. Experiment conditions: electrolyte, 0.1 M NBu_4ClO_4; TFA (proton source), 30 mM; [**3**], 1.3 mM; fixed potential, −0.95 vs SCE; WE, 0.9 mm graphite rods; CE graphite rod; WE, $Ag/AgNO_3$ (referenced internally to ferrocene).

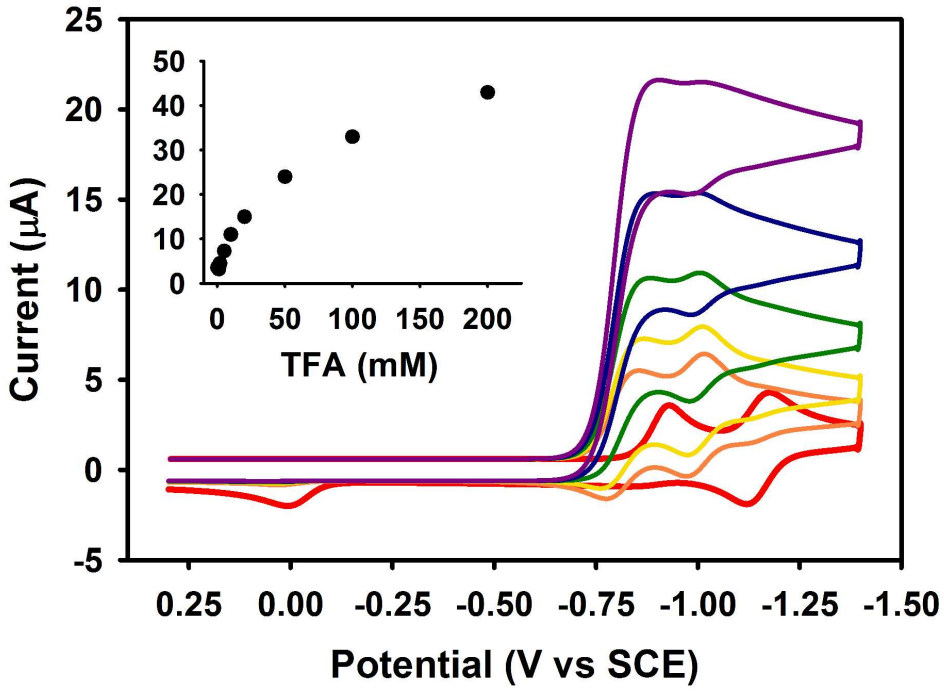

Figure S10. Simulated CVs of **3** in the presence of increasing [TFA]. Simulation parameters: [**3**] = 1 mM, [TFA] = 0-100 mM; scan rate = 100 mV/s; capacitance = 1×10^{-5} F. Kinetic and thermodynamic parameters listed in Scheme S2B.

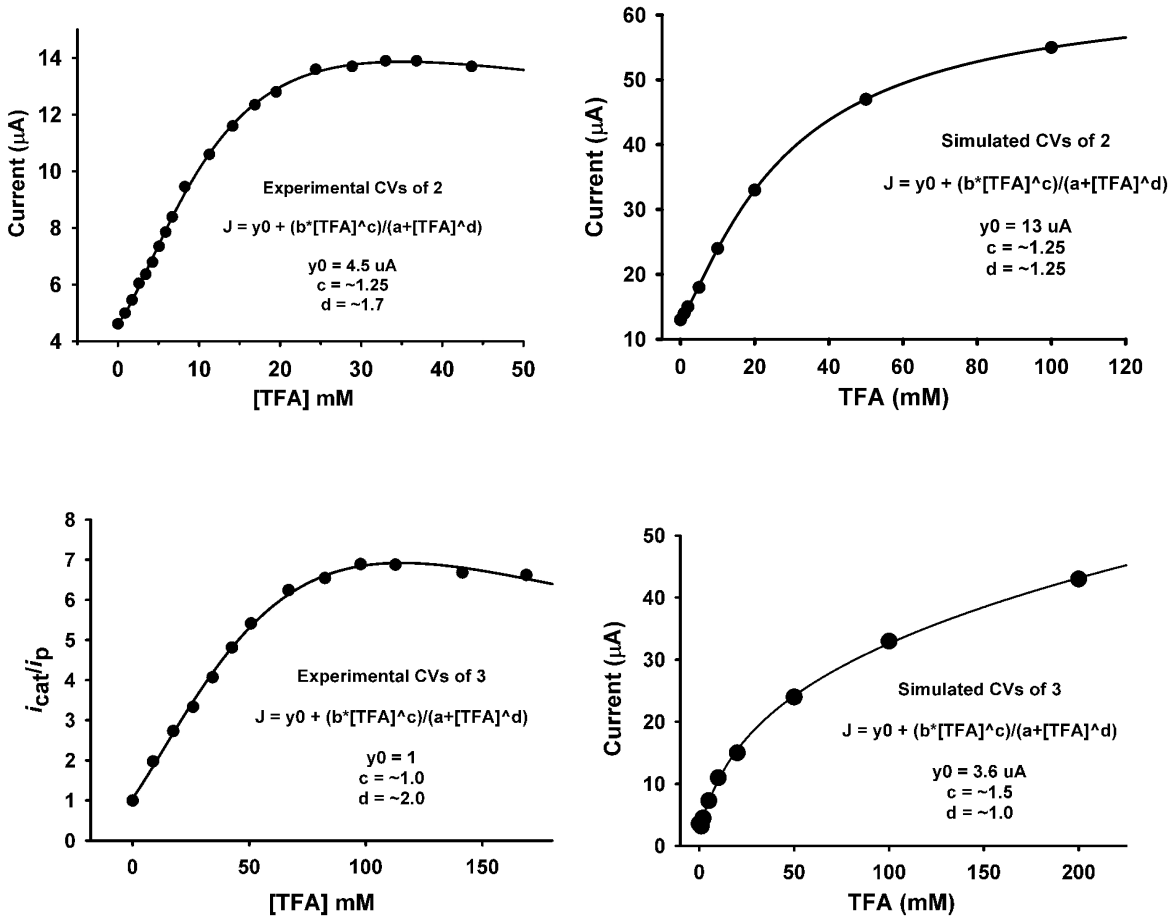

Figure S11. Curve fitting of experimental (in CH_2Cl_2) and simulated dependence of i_{cat} on [TFA] for **2** and **3**. Simulation parameters: [**3**] = 1 mM, scan rate = 100 mV/s; capacitance = 1×10^{-5} F. Kinetic and thermodynamic parameters listed in Schemes 1 and 2. ***Note:*** Concentrations of **2** and **3** in experiments were ~0.5 mM, while simulations were performed at catalyst concentrations of 1 mM, thus accounting for the difference in the simulated current values.

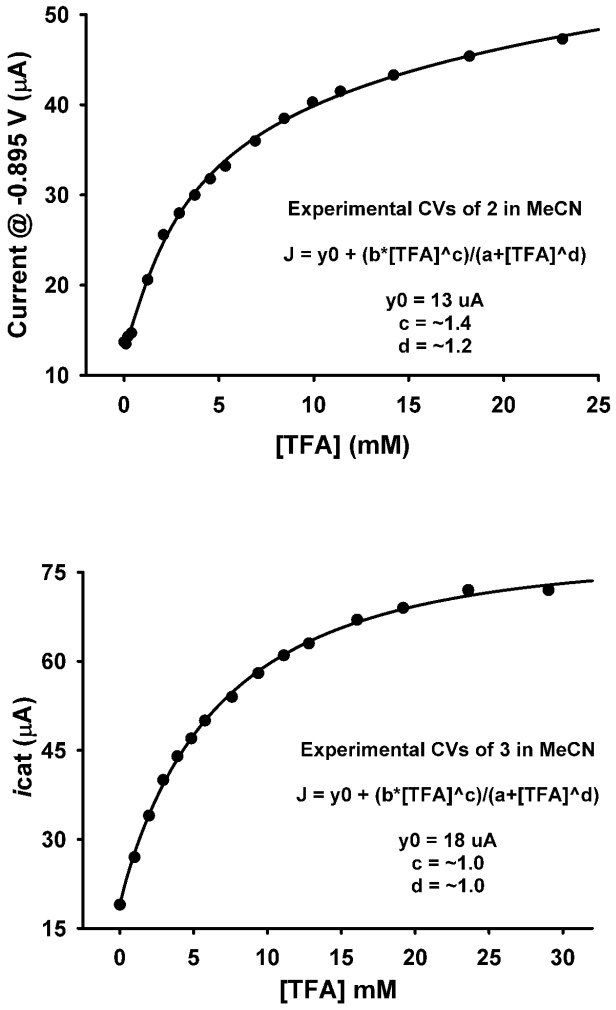

Figure S12. Same fitting procedure shown in Figure S11 for **2** and **3**, but with experimental data obtained in MeCN; [cat] = 1 mM in experiments and in simulations.

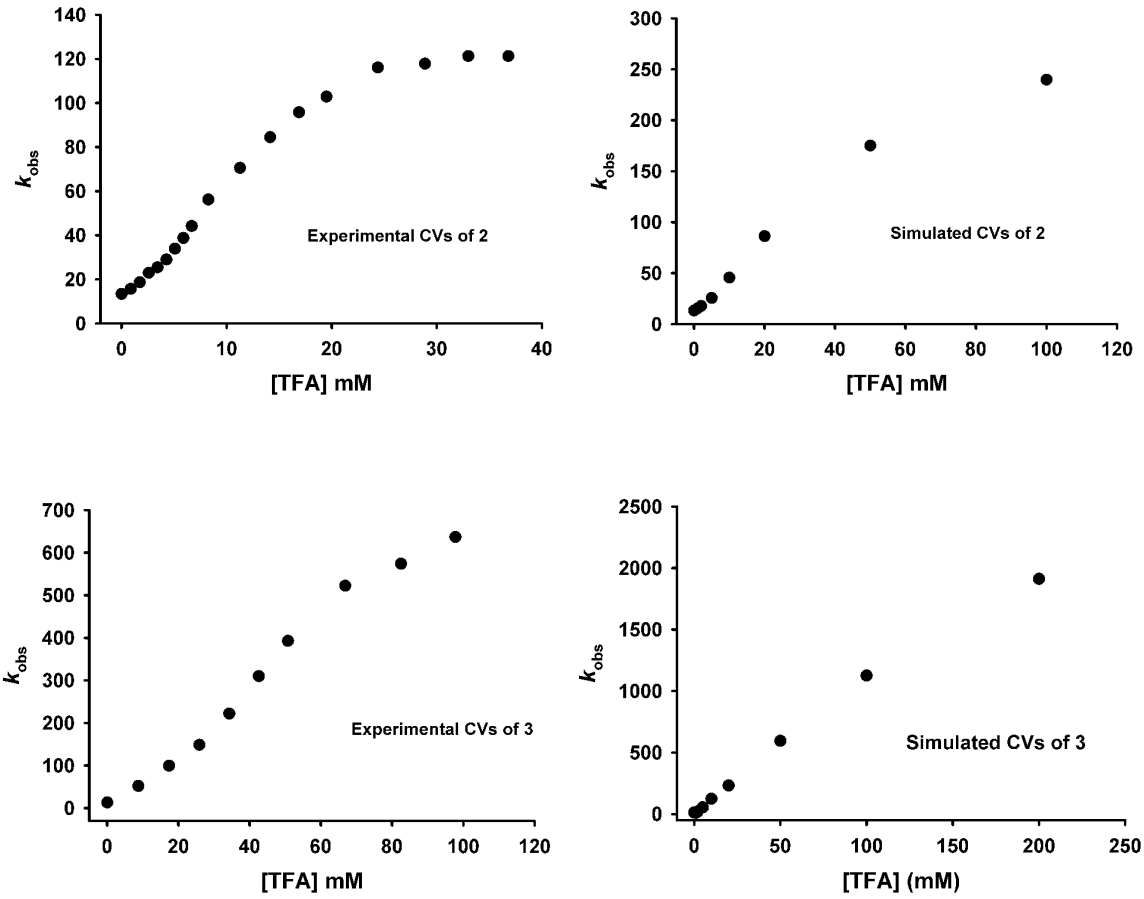

Figure S13. Plots of the experimental (in CH_2Cl_2) and simulated dependence of k_{obs} on [TFA] for **2** and **3**. Simulation parameters: [**3**] = 1 mM, scan rate = 100 mV/s; capacitance = 1×10^{-5} F. Kinetic and thermodynamic parameters listed in Schemes 1 and 2 (see manuscript reference 6e).

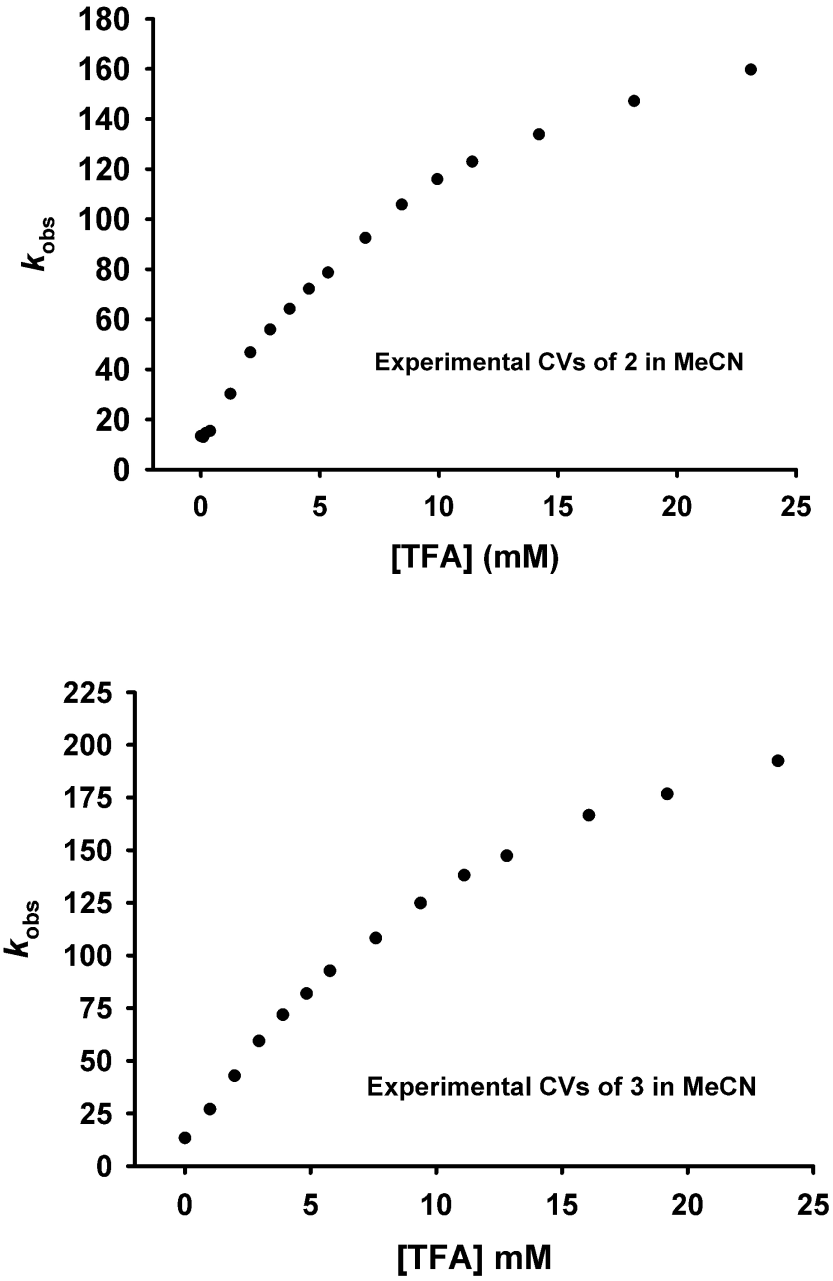

Figure S14. Plots of the experimental (in MeCN) dependence of k_{obs} on [TFA] for **2** and **3**. Simulation parameters: [**3**] = 1 mM, scan rate = 100 mV/s; capacitance = 1×10^{-5} F (see manuscript reference 6e).